High yield lactic acid selective oxidation into acetic acid over a Mo-V-Nb mixed oxide catalyst

Samadhan Lomate, Benjamin Katryniok, Franck Dumeignil, Sébastien Paul

Lomate et al. Sustainable Chemical Processes (2015) 3:5
DOI 10.1186/s40508-015-0032-7

SUSTAINABLE CHEMICAL PROCESSES

RESEARCH ARTICLE Open Access

High yield lactic acid selective oxidation into acetic acid over a Mo-V-Nb mixed oxide catalyst

Samadhan Lomate[1,2,3,4], Benjamin Katryniok[1,2,3], Franck Dumeignil[1,2,4,5] and Sébastien Paul[1,2,3*]

Abstract

In this paper, we report for the first time a one-pot reaction enabling total transformation of lactic acid to acetic acid over a Mo-V-Nb mixed oxide catalyst having an optimal atomic ratio 19:5:1. The mechanism of the reaction consists in two parallel ways leading to acetic acid: (i) oxi-dehydrogenation of lactic acid to pyruvic acid followed by decarboxylation and (ii) decarbonylation of lactic acid to acetaldehyde followed by oxidation. In the operating conditions we used, the catalyst is very active (total conversion of lactic acid) and selective towards acetic acid (100% selectivity). A 100% yield into acetic acid is hence obtained.

Keywords: Lactic acid, Acetic acid, Mo-V-Nb catalyst, Mixed oxide catalyst, Oxidation

Introduction

The announced depletion of oil along with the problem of global warming have shown up the urgent need for using processes based on bio-derived renewable resources for the production of fuels and starting materials of the chemical industry [1,2]. Most of these processes need a catalyst to orientate the reaction and accelerate its rate. Therefore, the development of new catalysts is of main importance to set up the processes of the tomorrow chemical industry that will make use of biomass-derived feedstocks [3]. As examples, the synthesis of hydrogen, of liquid fuels and of precursors for plastics from renewable resources, catalysis plays a very important role [4,5]. In this context, lactic acid, which is often referred as a "sleeping giant", has attracted much attention as an alternative resource for the production of important chemicals such as acrylic acid, 1,2-propanediol, 2,3-pentanedione, pyruvic acid, [6] acetaldehyde [7] and mainly the polylactic acid (PLA) polymer [8,9]. Lactic acid can be easily be obtained by fermentation of renewable sources such as sugars and starches or even waste streams (cheesy whey for instance) [10-12].

Acetic acid is a bulk chemical which is produced today in an amount exceeding 10 million tons per year worldwide [13]. It is one of the most used organic acids in the chemical industry [14]. The largest consumption of acetic acid is for the production of vinyl acetate [15], which is a monomer building block. About 33% of the world production of acetic acid in 2008 was used for the manufacture of vinyl acetate. The latter is mainly polymerized to polyvinyl acetate which finds application in paints and coatings or for poly vinyl alcohol and plastics. Acetic acid is furthermore employed in the synthesis of cellulose acetate, which is used to produce acetate fibres. Finally, acetic acid also finds application as food additives due to its role as acidity regulator.

As a matter of fact, nowadays more than 60% of the world acetic acid is produced by the carbonylation of petro-derived methanol [16]. On the other hand, the carbonylation method has a significant drawback due to catalyst solubility limitations and the loss of expensive Rh metal during the separation section. As an alternative, the biological transformation of lactic acid to acetic acid is well reported. Elferink et al. reported the conversion of lactic acid to acetic acid and 1,2-propanediol using *Lactobacillus buchneri* whereby one mole of lactic acid yielded equimolar amount of acetic acid and 1,2-propanediol [17]. Concerning the chemical conversion of lactic acid to acetic acid, the latter is notably reported as a side reaction in the oxidative dehydrogenation of lactic acid to pyruvic acid and dehydration of lactic acid to acrylic acid. For instance, Ai et al. obtained 9.2% yield

* Correspondence: sebastien.paul@ec-lille.fr
[1]Université Lille Nord de France, 59000 Lille, France
[2]CNRS UMR 8181, Unité de Catalyse et Chimie du Solide (UCCS), Cité Scientifique, Bâtiment C3, 59655 Villeneuve d'Ascq, France
Full list of author information is available at the end of the article

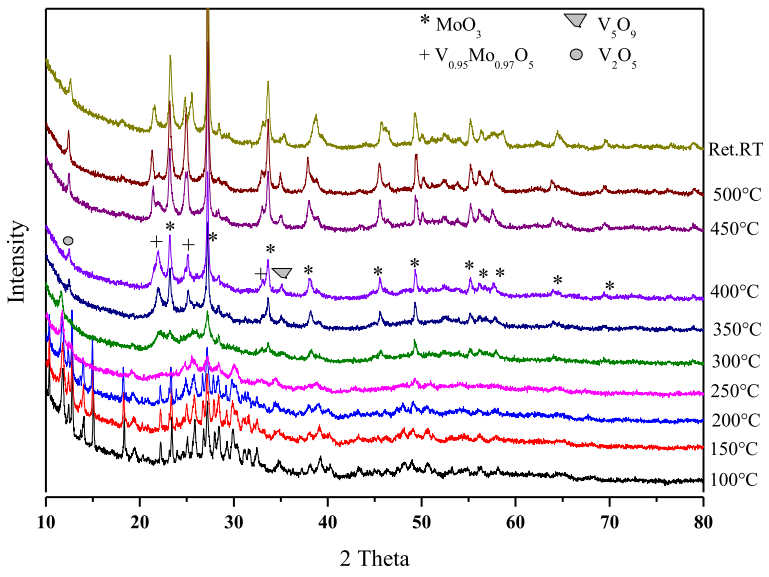

Figure 1 Temperature programmed XRD pattern of dry Mo-V-Nb.

in acetic acid form lactic acid using an iron phosphate catalyst doped with molybdenum [18]. The formation of acetic acid (0.7%) during dehydration of lactic acid was reported by Zhang et al. over NaY zeolite modified by alkali phosphate as a catalyst [19]. Tang et al. reported 1.3% acetic acid yield over barium phosphate catalysts in the lactic acid dehydration reaction [20]. Peng et al. observed 3.3% yield in acetic acid as a by-product in the barium sulphate catalysed dehydration of lactic acid [21]. Lingoes have reported the formation of 2% acetic acid in the lactic acid dehydration using barium based catalysts [22]. Much higher yield in acetic acid by chemo-catalysis were observed by Wang et al. from glucose via lactic acid using copper oxide catalyst (32%) [23]. Here, we report efficient and highly selective catalysts for the production of acetic acid. In this process, the catalytic oxidation of lactic acid is carried out over a multi-component Mo-V-Nb mixed oxide catalyst. To the best of our knowledge, this simple single-step catalytic process has not yet been reported and would provide a way to produce "green" acetic acid. The Mo-V-Nb is a versatile catalyst for the oxidative dehydrogenation. This catalyst mostly used in the oxidative dehydrogenation of ethane and propane [24,25]. The catalytic behaviour of this catalyst also investigated for the ammoxidation of propane to acrylonitrile [26-28]. The catalyst structure and catalytic properties of Mo-V-Nb catalyst also investigated for selective oxidation of propane to acrylic acid [29-31]. Mo-V-Nb oxide were examined in bulk and supported form for the oxidation of ethane to ethane and acetic acid [32].

Experimental

Catalyst synthesis

A molybdenum-vanadium-niobium mixed oxide catalyst with the following molar ratio Mo:V:Nb = 19:5:1 was prepared as follows: 10 mmol of niobium pentachloride (Aldrich 99%) were dissolved in water (50 mL), and ammonium hydroxide (Aldrich) was added until neutral pH was reached. The white precipitate (niobium hydroxide) was then filtered, washed with water and dissolved in a hot solution of oxalic acid dihydrate (50 mmol; Aldrich 99%). Then, an aqueous solution of ammonium metavanadate (50 mmol; Aldrich 99%) was added at 90°C followed by an aqueous solution of ammonium paramolybdate (27.14 mmol; Aldrich 99%). The obtained green slurry was heated under stirring until the water was evaporated. The residue was dried for 16 h at 120°C followed by a calcination step under static air at 400°C for 4 h (heating ramp 2°C/min).

Table 1 Textural, redox and acid properties of the Mo-V-Nb catalyst

BET surface area (m^2/g)	Pore volume (cm^3/g)	Pore size (Å)	Total acidity (mmol/g)	H_2 consumption mmol/g
10	0.022	31.5	0.161	6.47

Table 2 Atomic composition of the catalyst measured by XPS and XRF

Atomic ratio	Mo	V	Nb
Theoretical	19	5	1
XPS	19.1	4.6	1.2
XRF	16	3	1

Experimental set-up

The evaluation of the catalyst activity was carried out under atmospheric pressure in a gas phase down-flow fixed-bed reactor (stainless steel, 15 mm inner diameter, 180 mm length). 2 g of catalyst were loaded in the reactor and the remaining reactor volume was filled with SiC (VWR, 0.5 mm) to avoid the presence of any dead volume. The lactic acid (LA) aqueous solution (20 wt.%) was fed by a HPLC pump at a flow-rate of 3 mL/h, pre-vaporized at 190°C and diluted with air (30 mL/min STP). The resulting feed molar composition was 0.6:13.3:1 (LA: H_2O:Air) (GHSV = 3075 h^{-1}). The reaction temperature was varied between 250 and 300°C. The products were collected in a cold trap filled with water at 3°C and the analysis of the collected liquid was performed by HPLC on a Phenomenex column (ROA, organic acid H+; 300 × 7.8 mm). Sulphuric acid (5 mmol/L) was used as a mobile phase at a flowrate of 0.450 mL/min and the products were detected on a Shodex RI-101 detector at 35°C. The conversion of lactic acid and selectivity of products were calculated as follows:

$$\text{Selectivity}, \% = \frac{\text{Moles of acetic acid formed}}{\text{Moles of lactic acid reacted}} * 100 \quad (1)$$

$$\text{Conversion}, \% = \frac{\text{Moles of LA fed} - \text{Moles of LA recovered}}{\text{Moles of LA fed}} * 100 \quad (2)$$

The carbon balance was always found greater than 91%. Blank tests were done at 250°C using SiC only. No conversion was observed for lactic acid.

Catalyst characterization

The Mo-V-Nb oxide catalyst was characterised by different physico-chemical techniques, as described in the followings. Powder in-situ temperature X-ray diffraction measurement was performed (RT to 500°C) on a Bruker D8 advance diffractometer, using the CuKα radiation (λ = 1.5506 Å) as an X-ray source, in the 2θ range of 10-80° with steps of 0.02° per second. The composition and oxidation state of the elements present on the catalyst surface was determined by X-ray photoelectron spectroscopy (XPS). The XPS experiments were performed on a KRATOS Ultra instrument using a hemispherical energy analyzer. Monochromatic AlKα X-rays ($h\nu$ = 1486 eV) were used as the excitation

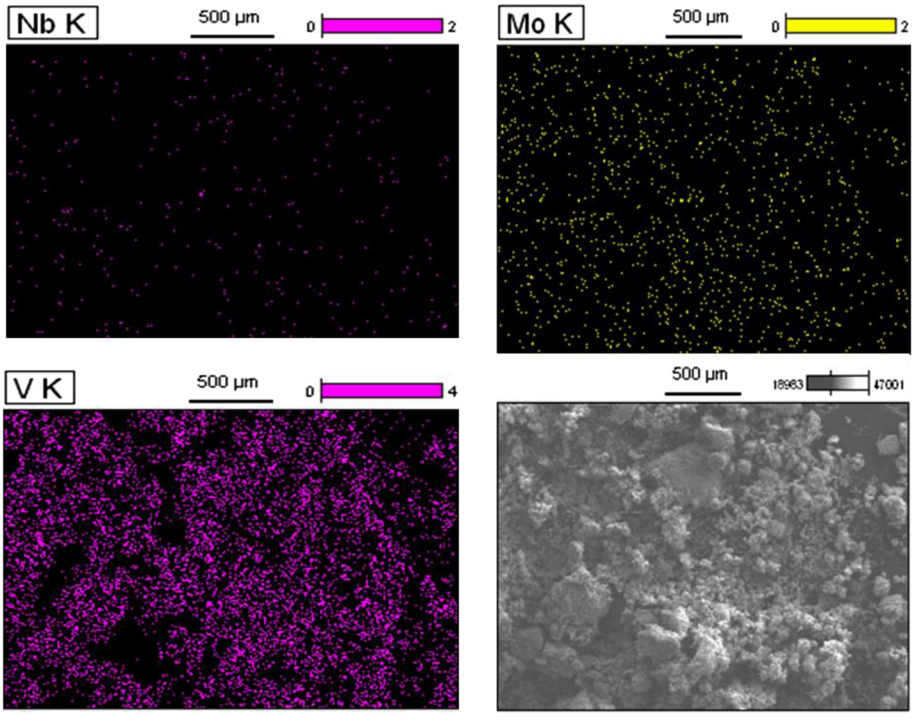

Figure 2 EDX mapping on the Mo-V-Nb catalyst.

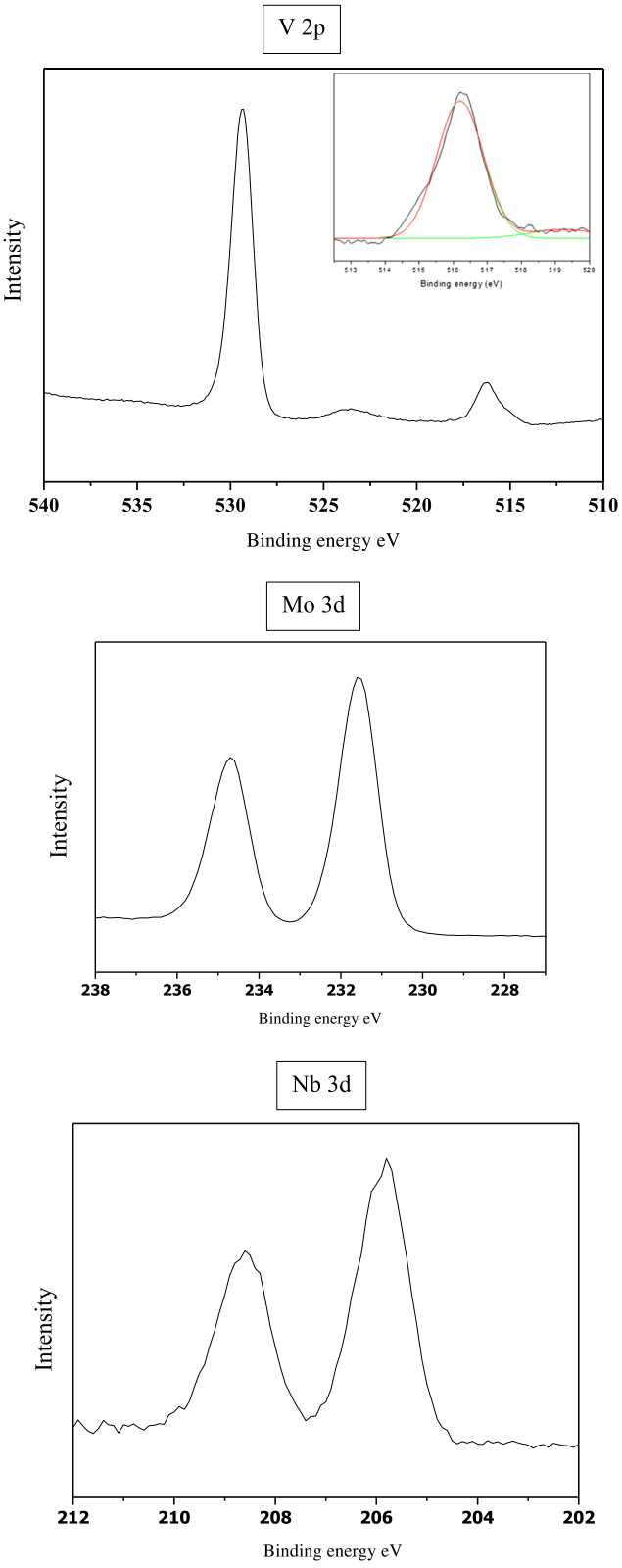

Figure 3 XPS spectra of the Mo-V-Nb catalyst.

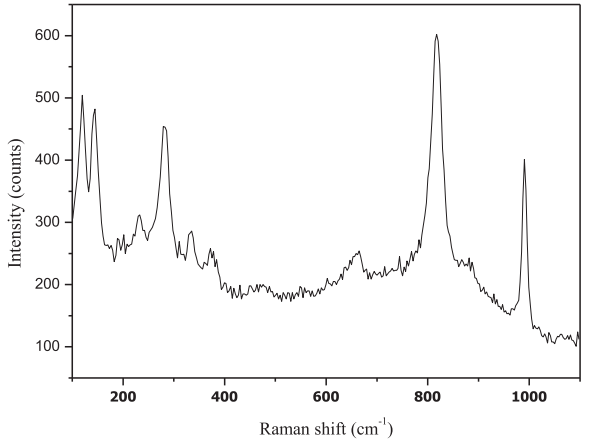

Figure 4 Raman spectra of the Mo-V-Nb catalyst.

source. The source was operated at 150 W. All the spectra were acquired at normal incidence, takeoff angle set at 90°, with the charge neutralizer switched on. The base pressure of the instrument was maintained at less than 6.66×10^{-13} bar. All the survey scans were collected with a pass energy of 160 eV and a step size of 1 eV/step while thigh-resolution spectra were collected with a pass energy of 40 eV and a step size of 0.1 eV/step. All the binding energies were referenced to the carbon 1 s CH*x* component set to 285 eV.

Ammonia temperature-programed desorption (NH_3-TPD) was carried out to measure the surface acidity of the catalyst. First, 50 mg of catalyst were treated under helium flow (30 mL/min) at 250°C for 2 h. After the pre-treatment, the catalyst was saturated with ammonia at 130°C using pulse-wise injection. Finally, NH_3-TPD desorption was carried out in helium at a heating rate of 10°C/min within the temperature range of 130 to 700°C. The signal was recorded by a thermo-conductive detector (TCD).

For the elemental analysis by energy dispersive X-Ray Fluorescence (XRF) a M4 Tornado from Bruker was employed. This tool is used for element characterization using small-spot Micro X-ray Fluorescence (Micro-XRF) analysis. For each sample 30 points were measured for in order to cover whole sample surface, with spot sizes of 200 μm for each point.

The atomic composition of the catalyst was further evaluated by EDX analysis. Elemental analysis was performed by energy dispersive X-ray spectroscopy on a Hitachi S3600N electron microscope equipped with a Thermo Ultradry EDX detector using an acceleration voltage of 30 kV.

The specific surface area and pore volume of the catalyst were measured through nitrogen adsorption at the liquid nitrogen temperature (77 K) using a Micrometrics ASAP 2010 instrument. The specific surface area (S_{BET}) was evaluated by using the multi-point BET method, while the pore size distribution was calculated according to the Barrett–Joyner–Halenda (BJH) formula applied to the desorption branch. The total pore volume (Vp) was calculated using the isotherms at the relative pressure (P/P_0) of 0.98.

The reducibility of the catalysts was evaluated by temperature-programmed reduction (TPR) using gaseous hydrogen as reducing agent. A typical experiment was performed with 100 mg of catalyst loaded into a quartz reactor and pre-treated in a He flow (30 mL/min) at 100°C for 2 h. Afterwards, the catalyst was heated from 100°C to 700°C (heating rate of 5°C/min) under the reductive gas H_2/He (5 mol.% H_2 in He; 30 mL/min). The effluent gas was analysed by a thermal conductivity detector (TCD).

Raman measurements were performed on a HORIBA HT Raman with a confocal microscope Raman system using an excitation wavelength of 532 nm supplied by a Renishaw HPNIR laser (10 mW). The Raman spectra were collected at room temperature in air in the region of 100–1100 cm^{-1}.

Table 3 Catalytic performance of Mo-V-Nb catalyst

	LA conversion (%)	Selectivities (%)		
		Pyruvic acid	Acetaldehyde	Acetic acid
200°C	80	32	13	55
225°C	90	20	13	67
250°C	100	0	0	100

Conditions: 2 g cat., GHSV 3075 h^{-1}, ratio LA:H_2O:Air 0.6:13.3:1.

Results and discussion

Catalyst characterization

XRD of the dried Mo-V-Nb catalyst was performed in the range of 100 -500°C and the pattern are shown in Figure 1. From the observed patterns one can see that all nitrate species were decomposed at 400°C, meaning that he employed calcination temperature of 400°C was sufficient to obtain metal oxide species. Intense characteristic peaks were observed for the α-MoO_3 orthorhombic phase [33]. On the other hand, no signals were detected for niobium species. This can be explained by i) the low content of niobium compared to molybdenum (Mo:V:Nb = 19:5:1), ii) the formation of microcrystals, iii) the formation of amorphous phases [34]. In fact, for niobium oxide, the formation of an amorphous phase was reported for a calcination at >400°C [35,36]. Concerning vanadium, small peaks for V_5O_9 and V_2O_5 [JCPDS 18–1450, 45–1074] was observed, accompanied with mixed oxide phases of vanadium and molybdenum $V_{0.95}Mo_{0.97}O_5$ [JCPDS 50–0535] [26].

The textural properties were determined by nitrogen physisorption. The specific surface of the catalyst was 10 m^2/g with a pore volume of 0.022 cm^3/g and an

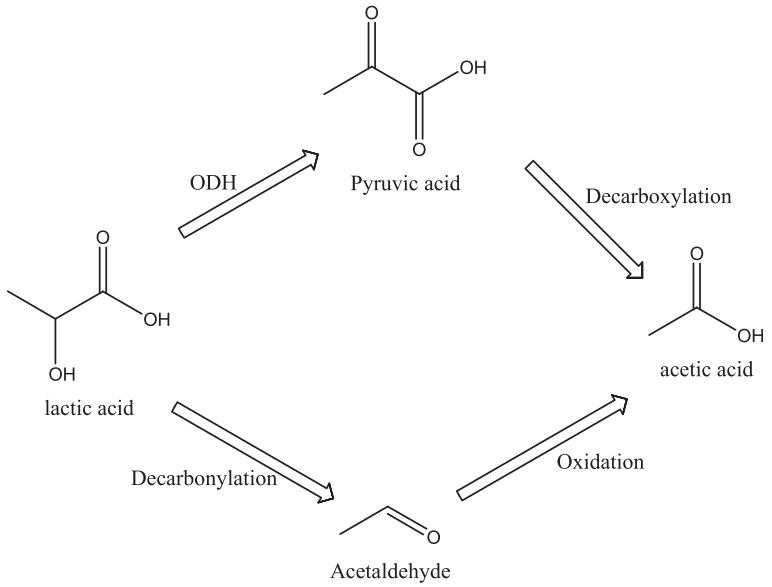

Figure 5 Proposed pathway for the acetic acid formation from lactic acid.

average pore diameter of 3 nm, which is characteristic for a classical bulk catalyst.

The amount of acid sites determined by ammonia TPD is presented in Table 1. The catalyst shows two peaks of ammonia desorption, one at low temperature (between 200 and 400°C) - corresponding to weak acid sites - and another one at high temperature (700°C) corresponding to strong acid sites. The quantification clearly indicates that the majority of sites were weak (0.101 mmol/g) rather than strong (0.06 mmol/g).

The reducibility was also studied using temperature-programmed reduction (TPR). The results are reported in Table 1. The reduction peak of the Mo-V-Nb catalyst occurred at high temperature (650°C) and showed a hydrogen consumption of 6.47 mmol/g.

The atomic compositions of the bulk and of the surface of the catalyst were measured by XRF and XPS respectively (Table 2). From the results, one can see that the bulk elemental ratio determined by XRF shows a slightly lower content of vanadium (3), whereas the surface elemental ratio is nearly identical (4.6) to the theoretical value (5). Similar observations can be drawn up for the molybdenum content determined by XRF which is again lower than the theoretical value (16% vs. 19%). On the other hand, for XPS and XRF, the experimental niobium content is exactly the same as the theoretical one.

The distribution of the elements was verified by EDX mapping. The corresponding images are shown in Figure 2. From the images it is clear that the niobium content is low, but the distribution is nevertheless uniform. The same conclusion can be drawn for molybdenum and vanadium, which are homogeneously dispersed in the catalyst.

XPS was employed to determine the oxidation states of Mo, V and Nb from the respective binding energies, as shown in Figure 3. For molybdenum (Mo 3d peak), the binding energies were 235.1 eV ($3d_{3/2}$) and 231.9 eV ($3d_{3/2}$) corresponding to the exclusive presence of Mo^{+VI} oxidation state [37]. For vanadium (using the V $2p_{3/2}$ signal), the binding energy peak at 516 eV is ascribed to V^{+4} whereas the peak at 518 eV corresponds to V^{+5}. The deconvolution of the V $2p_{3/2}$ peak showed that 94% of vanadium are in V^{+4} state and 6% in V^{+5} [38,39]. Finally, the niobium was exclusively in the Nb^{+V} oxidation state with a binding energy of 206.1 eV corresponding to Nb $3d_{3/2}$ [40,41].

Raman spectra of calcined Mo-V-Nb catalyst were recorded to determine the metal species in the catalyst. The pattern for the Raman spectra is shown in Figure 4, The phases observed by XRD were also confirmed by Raman spectroscopy. In fact, the catalyst shows characteristic peaks at 139 and 282 cm^{-1} for the orthorhombic vanadium oxide (V_2O_5) [42,43]. For the orthorhombic MoO_3, more intense characteristic peaks are observed at 114, 129, 281, 665, 819 and 997 cm^{-1} [44,45].

Catalytic activity

The catalytic activity of the Mo-V-Nb catalyst was investigated in the temperature range of 200-250°C. From the results (Table 3), one can see that the conversion increased from initially 80% (200°C) to full conversion at 250°C. The main product was always acetic acid with even 100% selectivity at 250°C. At lower temperatures, the other observed products were pyruvic acid and acetaldehyde. The selectivity to acetaldehyde remained

constant at 200°C and 225°C (13%), but decreased to 0% at the increased temperature of 250°C. The selectivity to pyruvic acid followed the same trend since it decreased from 32% at 200°C to 20% at 225°C, and then dropped to 0% at 250°C, meaning that both are potential intermediates for the formation of acetic acid.

Concerning the reaction mechanism, the one-step reaction of lactic acid to acetic acid can proceed *via* two parallel pathways, namely i) the decarbonylation to acetaldehyde and consecutive oxidation of the latter to acetic acid and ii) the oxidative dehydrogenation (ODH) to pyruvic acid with consecutive decarboxylation of the latter to acetic acid (Figure 5) [46]. Both pathways seem possible over a bi-functional catalyst exhibiting redox and acidic properties – as Mo-V-Nb does. In fact, Desponds et al. already demonstrated that Mo-V-Nb is a very efficient catalyst for the oxidative dehydrogenation of ethane with 77% selectivity for ethylene at 7% conversion [47]. On the other hand, Iglesias et al. demonstrated that Mo-V-Nb was also highly active in the oxidation of ethanol to acetic acid [48]. In order to provide proof, an additional reaction was performed using acetaldehyde as reactant over Mo-V-Nb at 250°C. The corresponding reaction showed a selectivity of 89% for acetic acid at full conversion of acetaldehyde. These results strongly suggest that the formation of acetic acid from lactic acid proceeds via decarboxylation/decarbonylation to acetaldehyde, followed by the oxidation of the latter to acetic acid.

Conclusion

In the present work, a Mo-V-Nb mixed oxide catalyst having an atomic ratio of 19:5:1 was synthesized and used for the direct oxidation of lactic acid to acetic acid. The catalyst was extensively characterized by nitrogen adsorption-desorption, XRD, EDX, XRF, XPS, TPR and ammonia TPD. The results show that the Mo-V-Nb mixed oxide catalyst presents both redox and acid properties enabling the parallel formation of acetaldehyde and pyruvic acid as intermediates, which give acetic acid at higher lactic acid conversion. Thus at 250°C, a remarkable yield into acetic acid is obtained (100%).

Competing interests

The authors declare that they have no competing interests.

Authors' contributions

SL carried out the catalyst synthesis, the catalytic tests and the characterizations. BK, FD and SP contributed to the interpretation of the results and the experimental design. All authors read and approved the final manuscript.

Author details

[1]Université Lille Nord de France, 59000 Lille, France. [2]CNRS UMR 8181, Unité de Catalyse et Chimie du Solide (UCCS), Cité Scientifique, Bâtiment C3, 59655 Villeneuve d'Ascq, France. [3]Ecole Centrale de Lille, (ECLille), Cité Scientifique, CS 20048, 59651 Villeneuve d'Ascq, France. [4]Université Lille 1 (USTL), Cité Scientifique, 59650 Villeneuve d'Ascq, France. [5]Institut Universitaire de France (IUF), Maison des Universités, 103 Boulevard Saint-Michel, 75005 Paris, France.

Received: 2 September 2014 Accepted: 8 April 2015
Published online: 21 April 2015

References

1. Huber GW, Iborra S, Corma A. Synthesis of transportation fuels from biomass: chemistry, catalysts and engineering. Chem Rev. 2006;106:4044.
2. Huber GE, Corma A. Synergies between bio- and oil refineries for the production of guels from biomass. Angew Chem Int Ed. 2007;46:7184.
3. Corma A, Iborra S, Velty A. Chemical routes for the transformation of biomass into chemicals. Chem Rev. 2007;107:2411.
4. Huber GW, Chheda JN, Barrett CJ, Dumesic JA. Production of liquid alkanes by aqueous-phase processing of biomass-derived carbohydrates. Science. 2005;308:1446.
5. Huber GW, Cortright RD, Dumesic JA. Renewable alkanes by aqueous-phase reforming of biomass-derived oxygenates. Angew Chem Int Ed. 2004;43:1549.
6. Lomate S, Bonnotte T, Paul S, Dumeignil F, Katryniok B. Synthesis of pyruvic acid by vapour phase catalytic oxidative dehydrogenation of lactic acid. J Mol Cat A Gen. 2013;377:123–8.
7. Katryniok B, Paul S, Dumeignil F. Highly efficient catalyst for decarbonylation of lactic acid to acetaldehyde. Green Chem. 2010;12:1910–3.
8. Dusselier M, Van Wouwe P, Dewaele A, Makshina E, Sels BF. Lactic acid as a platform chemical in the biobased economy: the role of chemocatalysis. Energ Environ Sci. 2014;6:1415.
9. Fan Y, Zhou C, Zhu X. Selective catalysis of lactic acid to produce commodity chemicals. Catal Rev. 2009;51:293.
10. Jarvinen M, Myllykoski L, Keiski R, Sohlo I. Separation of lactic acid from fermented broth by reactive extraction. J Bioseparation. 2000;9:163.
11. Timmer JMK, Kromkamp J, Robbertsen T. Lactic-acid separation from fermentation broths by reverse-osmosis and nanofiltration. J Membr Sci. 1994;92:185.
12. Tejayadi S, Cheryan M. Lactic acid from cheese whey permeate. Productivity and economics of a continuous membrane bioreactor. Appl Microbiol Biotechnol. 1995;43:242.
13. Vossa B, Schjødt NC, Grunwaldt JD, Andersen SI, Woodley JM. Kinetics of acetic acid synthesis from ethanol over a Cu/SiO2 catalyst. Appl Catal A Gen. 2011;402:69.
14. Bala S. Chemicals Economic Handbook. Menlo Park, CA: SRI International; 2003. p. 602.
15. Han YF, Kumar D, Sivadinarayana C, Goodman DW. Kinetics of ethylene combustion in the synthesis of vinyl acetate over a Pd/SiO2Catalyst. J Catal. 2004;224:60.
16. Yoneda N, Kusano S, Yasui M, Pujado P, Wilcher S. Recent advances in processes and catalysts for production of acetic acid. Appl Catal A Gen. 2001;221:253–65.
17. Oude Elferink S, Krooneman J, Gottschal J, Spoelstra S, Faber F, Driehuis F. Anaerobic conversion of lactic acid to acetic acid and 1,2-propanediol by lactobacillus buchneri. Appl Environ Microbiol. 2001;67:125–32.
18. Ai M. Catalytic activity of iron phosphate doped with a small amount of molybdenum in the oxidative dehydrogenation of lactic acid to pyruvic acid. Appl Catal A Gen. 2002;234:235.
19. Zhang J, Zhao Y, Pan M, Feng X, Ji W, Au C. Efficient acrylic acid production through bio lactic acid dehydration over NaY zeolite modified by alkali phosphates. ACS Catal. 2011;1:32–41.
20. Tang C, Peng J, Fan G, Li X, Pu X, Bai W. Catalytic dehydration of lactic acid to acrylic acid over dibarium pyrophosphate. Catal Comm. 2014;43:231–4.
21. Peng J, Li X, Tang C, Bai W. Barium sulphate catalyzed dehydration of lactic acid to acrylic acid. Green Chem. 2014;16:108–11.
22. Lingoes J, Collias D. Catalytic conversion of lactic acid to acrylic acid, US. 2013;0274514 A1
23. Wang Y, Jin F, Sasaki M, Wahyudiono, Wang F, Jing Z, et al. Selective conversion of glucose into lactic acid and acetic acid with copper oxide under hydrothermal conditions. AIChE J. 2013;59:6.
24. Ruth K, Burch R, Kieffery R. Mo–V–Nb oxide catalysts for the partial oxidation of ethane. J Catal. 1998;175:27–39.
25. Solsona B, Vázquezb MI, Ivars F, Dejoz A, Concepción P, López Nieto JM. Selective oxidation of propane and ethane on diluted Mo–V–Nb–Te mixed-oxide catalysts. J Catal. 2007;252:271–80.
26. Guerrero-Pérez M, Al-Saeedi J, Guliants V, Bañares M. Catalytic properties of mixed Mo-V-Sb-Nb-O oxides catalysts for the ammoxidation of propane to acrylonitrile. Appl Catal A Gen. 2004;260:93–9.

27. Kubo J, Watanabe N, Ueda W. Propane ammoxidation with lattice oxygen of Mo–V–O-based complex metal oxide catalysts. Chem Eng Sci. 2008;63:1648–53.
28. Wang G, Guoa Y, Lu G. Promotional effect of cerium on Mo–V–Te–Nb mixed oxide catalyst for ammoxidation of propane to acrylonitrile. Fuel Process Technol. 2015;130:71–7.
29. Al-Saeedi J, Guliants V, Guerrero-Pérez O, Bañares M. Bulk structure and catalytic properties of mixed Mo–V–Sb–Nb oxides for selective propane oxidation to acrylic acid. J Catal. 2003;215:108–15.
30. Gaffney AM, Chaturvedi S, Clark Jr MB, Han S, Le D, Rykov SA, et al. Characterization and catalytic studies of PVD synthesized Mo/V/Nb/Te oxide catalysts. J Catal. 2005;229:12–23.
31. Seok Oh K, Ihl Woo S. Effect of preparation and reaction condition on the catalytic performance of Mo thTe–Nb catalysts for selective oxidation of propane to acrylic acid by high-throughput methodology. Catal Today. 2008;137:61.
32. Li X, Iglesia E. Support and promoter effects in the selective oxidation of ethane to acetic acid catalyzed by Mo-V-Nb oxides. Appl Catal A. 2008;334:339–47.
33. Kido A, Iwamoto H, Azuma N, Ueno A. Effects of catalyst heating rates upon the activity of silica-supported silicomolybdic acid catalysts for methane partial oxidation. Catal Surv Asia. 2002;6:45.
34. Botella P, López Nieto JM, Dejoz A, Vázquez MI, Martinez-Arias A. Mo-V-Nb mixed oxide as catalyst in the selective oxidation of ethane. Catal Today. 2003;78:507.
35. Paulis M, Martin M, Soria DB, Diaz A, Odriozola JA, Montes M. Preparation and characterization of niobium oxide for the catalytic aldol condensation of acetone. Appl Catal A Gen. 1999;180:411.
36. Chai SH, Wang HP, Liang Y, Xu BQ. Sustainable production of acrolein: gas-phase dehydration of glycerol over Nb2O5 catalyst. J Catal. 2007;250:342.
37. Wagner JB, Timpe O, Hamid FA, Trunschke A, U W, Su DS, et al. Surface texturing of Mo–V–Te–Nb–Ox selective oxidation catalysts. Top Catal. 2006;38:51–8.
38. Albonetti S, Cavani F, Trifiro F, Venturoli P, Calestani G, Lopez Granados M, et al. A comparison of the reactivity of "nonequilibrated" and "equilibrated" V–P–O catalysts: structural evolution, surface characterization, and reactivity in the selective oxidation of*n*-butane and*n*-pentane. J Catal. 1996;160:52.
39. Delishere P, Bere KE, Abon M. Vanadyl pyrophosphate catalysts: surface analysis by XPS and LEIS. Appl Catal A Gen. 1998;172:295.
40. Asakura K, Nakatani K, Kubota T, Iwasawa Y. Characterization and kinetic studies on the highly active ammoxidation catalyst MoVNbTeOx. J Catal. 2000;194:309–17.
41. Baca M, Pigamo A, Dubois JL, Millet JMM. Propane oxidation on MoVTeNbO mixed oxide catalysts: study of the phase composition of active and selective catalysts. Top Catal. 2003;23:39–46.
42. Castriota M, Cazzanelli E, Fasanella A, Teeters D. Electrical conductivity and Raman characterization of V2O5 grown by sol–gel technique inside nanoscale pores. Thin Solid Films. 2014;553:127–31.
43. Rodella CB, Nascente PAP, Mastelaro VR, Zucchi MR, Franco RWA, Magon CJ, et al. Chemical and structural characterization of V_2O_5/TiO_2 catalysts. J Vac Sci Technol A. 2001;19:1158–63.
44. Holmes SA, Al-Saeedi J, Guliants VV, Boolchand P, Georgiev D, Hackler U, et al. Solid state chemistry of bulk mixed metal oxide catalysts for the selective oxidation of propane to acrylic acid. Catal Today. 2001;67:403–9.
45. Shen L, Yin H, Wang A, Lu X, Zhang C. Gas phase oxidehydration of glycerol to acrylic acid over Mo/V and W/V oxide catalysts. Chem Eng J. 2014;244:168–77.
46. Brown BR. The mechanism of thermal decarboxylation. Rev Chem Soc. 1951;5:131.
47. Desponds O, Keiski RL, Somorjai GA. The oxidative dehydrogenation of ethane over molybdenum-vanadium-niobium oxide catalysts: the role of catalyst composition. Catal Lett. 1993;19:17.
48. Li X, Iglesias E. Selective catalytic oxidation of ethanol to acetic acid on dispersed Mo-V-Nb mixed oxides. Chem Eur J. 2007;13:9324.